Instruments and Methods

Glaciological and volumetric mass-balance measurements: error analysis over 51 years for Glacier de Sarennes, French Alps

E. THIBERT,[1] R. BLANC,[2] C. VINCENT,[2] N. ECKERT[1]

[1]Unité de Recherche ETNA (Cemagref), 2 rue de la Papeterie, BP 76, 38402 Saint-Martin-d'Hères Cedex, France
E-mail: emmanuel.thibert@cemagref.fr
[2]Laboratoire de Glaciologie et de Géophysique de l'Environnement du CNRS (associé à l'Université Joseph Fourier – Grenoble I), 54 rue Molière, BP 96, 38402 Saint-Martin-d'Hères, France

ABSTRACT. The mass balance of Glacier de Sarennes, French Alps, has been measured since 1949, using the glaciological method based on core and ablation stake data, and area extrapolations, to find the overall glacier balance. The cumulative balance obtained in this way is very dependent on systematic errors that can increase linearly with the number, N, of measurement years, whereas random errors rise with $\sqrt{N}$. The volumetric-balance method based on aerial photogrammetry provides results whose errors do not depend on the number of years. This method was used to test field measurements for the period 1952–2003 and gives a mass balance of -32.30 ± 1.04 m w.e. compared to -34.89 ± 1.15 m w.e. based on field data. The discrepancy between the two methods is discussed on the basis of a careful error analysis. Moreover, the possibility of using the volumetric method to detect biases in field measurements is evaluated in terms of two types of errors. The number and locations of measurement sites required to account for all the spatial and temporal variabilities of the mass balance is discussed by variance analysis. Methodological implications and recommendations are presented to provide mass-balance measurements of the best possible accuracy.

LIST OF SYMBOLS

(SD denotes standard deviation)

Volumetric mass balance

ρ, σ_ρ	Density in water equivalent conversion, SD
$Z(x,y)$	Altitude given by the digital elevation model
Δm_{vol}	Mass variation in the volumetric method
σ_{rgh}	Glacier surface roughness
$\sigma_{stereo.xy}, \sigma_{stereo.z}$	Planimetric, altimetric errors in the stereoscopic measurement
σ_{phot}	Sighting error on stereotypes
s	Scale of stereotypes
T	Focal length
B	Stereoscopic base
P	Number of points measured by photogrammetry
σ_z^i	Mean internal altimetric error
$\sigma_x, \sigma_y, \sigma_z$	Orientation residuals in planimetry and altimetry
$\sigma_{a.o}$	Uncertainty in altitudes due to orientation residuals
S_m, σ_s	Glacier mean surface area used for volume to net balance reduction, SD
b_{vol}, σ_{vol}	Mass balance given by the volumetric method, SD
σ_{sp}	Spatial variability of the mass balance

Glaciological mass balance

N	Number of years of measurements
n	Number of sampling sites
b_t	Yearly glacier-wide balance
S_t	Surface area of the glacier for year t
Δm_{gla}	Mass variation in the glaciological method
d, σ_d	Density of snow or firn, SD
$\sigma_{b-}^{ice}, \sigma_{b-}^{firn}$	Errors for negative balance in ice, firn
σ_{b+}	Error for a positive balance
σ_{samp}	Sampling error related to a finite number of sites
b_{gla}, σ_{gla}	Cumulative mass balance over the period, SD

Comparison and variance analysis

α, β	Type I and II error in statistical hypothesis tests
F	Normal law repartition function
δb	Detectable discrepancy at given type I and II errors
$b_{i,t}$	Mass balance at site i for year t
α_i, β_t	Spatial and temporal components
$\gamma_i \delta_t$	Non-linear cross-terms
$\varepsilon_{i,t}$	Residuals

INTRODUCTION

Objectives

Mountain-glacier mass balances are excellent indicators of climate change over the last few centuries (Oerlemans and Fortuin, 1992; Haeberli, 1995). However, the investigation of climate trends requires the measurement of mass balance over several decades (Vincent, 2002), and long series are also useful for the modelling of glacier dynamics (e.g. Le Meur and Vincent, 2003). Unfortunately, throughout the world, only 33 glaciers have annual mass-balance series longer than 40 years (Dyurgerov and Meier, 1999). Given the
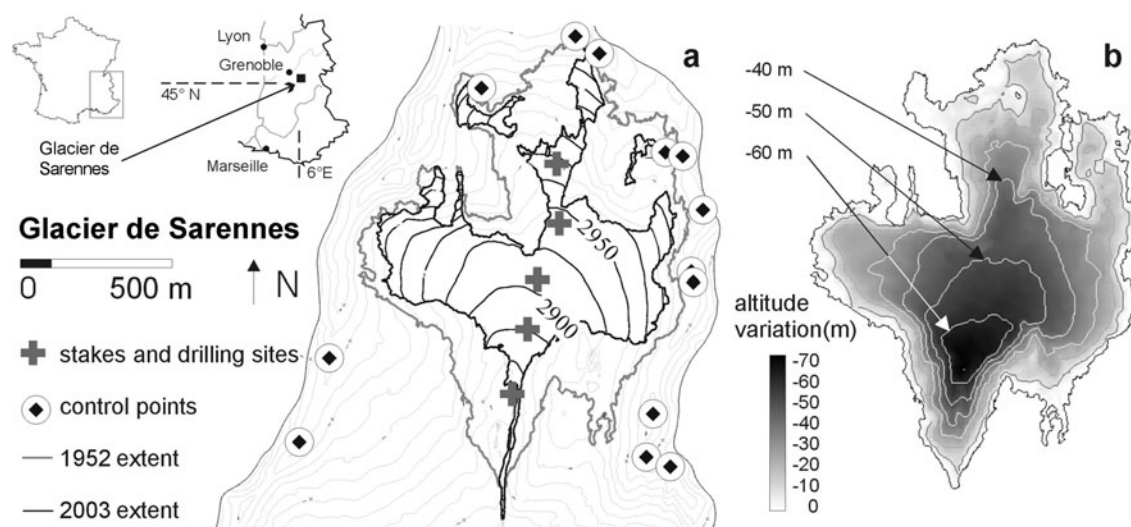
Fig. 1. (a) Location of stakes, drilling sites and control points used for photogrammetric restitution. Contour lines on bedrock and on the glacier are at 25 m intervals. (b) Spatial repartition of the 51 year altitude variations obtained from photogrammetry. Contour lines of altitude change are at 10 m intervals.

limited number of long balance series, the quality of such data is very important.

The traditional field-measurement method is the glaciological method, in which yearly point mass balances are obtained from stakes inserted in ice and from cores drilled in firn. When extrapolated to the whole surface of the glacier and added year after year, the resulting cumulative glacier-wide balance is likely to be very sensitive to systematic errors which accumulate linearly with the number of measurement years (denoted as N; see List of symbols). Such systematic errors will determine the exactness (veracity) of the method. Its precision (reproducibility) will depend on random errors that increase in the cumulative mass balance only with $\sqrt{N}$. Discerning these two types of errors requires an independent method for which the intrinsic error is as small as possible and not time-dependent.

The volumetric mass-balance method, in which changes in the surface elevation of a glacier are calculated from photogrammetry, can be used to this end, as its intrinsic errors are mostly random (Krimmel, 1999; Østrem and Haakensen, 1999; Cox and March, 2004). The comparison of measurements is a classical problem in metrology, requiring detailed error analysis to determine possible significant discrepancies within their natural scatter. Surprisingly, very few studies have focused on this point.

Previous studies

Meier and others (1971) indicated errors between ±0.1 and ±0.34 m w.e. for balances determined by the glaciological method. Lliboutry (1974) calculated an error of ±0.19 m w.e. for ablation measured with stakes, whereas Vallon and Leiva (1981) indicated ±0.3 m w.e. for mass balances obtained by drilling in the accumulation area. Most authors have proposed error estimates between ±0.2 and ±0.4 m w.e. (Braithwaite, 1986; Braithwaite and others, 1998; Cogley and Adams, 1998; Cox and March, 2004). In a recent study, Gerbeaux and others (2005) attempted to discern winter and summer balance measurements and their locations (accumulation/ablation areas). They estimated an error of ±0.10 m w.e. for ablation measured in ice and between −0.25 and +0.4 m w.e. for ablation measured in

firn. Errors owing to spatial sampling and to area integration have been investigated by Vallon and Leiva (1981). Using three integration methods, they concluded that the integration error is about ±0.07 m w.e. and the sampling error is approximately ±0.07 m w.e. The relation linking the measurement error at a site to the error in the glacier total balance has also been treated by Fountain and Vecchia (1999).

When assessing potential biases related to the sampling and area-integration method, it is of interest to compare results with the balance obtained from maps, given that photogrammetry integrates the overall spatial variability. Several studies have undertaken such a comparison and provided estimates of the error in the volumetric method (Krimmel, 1999; Andreassen, 1999; Cox and March, 2004). The reported errors are consistent, about ±1 to 2 m w.e., depending on map quality and photograph condition. Only Krimmel (1999) reports a significant discrepancy between the two types of measurements and suggests the water-equivalent conversion and the area integration as possible sources of bias.

Here we compare the two methods based on the long mass-balance series of Glacier de Sarennes, France (45°07′ N; 6°07′ E; Fig. 1) initiated in 1949. Preceding studies show a discrepancy of 18% (Valla and Piedallu, 1997). This led us to carry out a new estimate of the volumetric mass balance together with a careful error analysis that is also developed for field data. Possible sources of systematic errors are discussed by a variance analysis.

VOLUMETRIC MASS BALANCE

Principle of calculation

In this method, digital elevation models (DEMs) of the glacier are subtracted to calculate volume changes. The volumetric balance calculation between two dates (initial state 1, final state 2) requires knowledge of the altitude, $Z(x, y)$, of the glacier and the bedrock margins that may have been covered or uncovered. Calculations also require the density function, $\rho(x, y, z)$, so the water-equivalent mass of the glacier at date 1 (covering the space S1) will be

Table 1. Characteristics of the aerial photographs

	Date	
	1 August 1952	20 September 2003
Scale at mean altitude	1/31 090	1/20 414
Focal length (mm)	124.670	153.420
Stereotype size (mm)	190 × 190	240 × 240
Stereoscopic base (km)	1.722	1.522

expressed as:

$$m_1 = \iint_{S1} \left[\int_{Z_0(x,y)}^{Z_1(x,y)} \rho_1(x,y,z)\, dz \right] dx\, dy, \qquad (1)$$

where subscript 0 refers to the glacier bedrock and 1 to initial state 1. As the density function is generally unknown, we apply Sorge's law and accordingly assume that the density remains constant between two dates (i.e. $\rho_1 = \rho_2 = \rho$; Bader, 1954), so the mass variation, Δm_{vol} can be written as:

$$\Delta m_{vol} = m_2 - m_1 = \iint_{S1 \cup S2} \left[\int_{Z_1(x,y)}^{Z_2(x,y)} \rho(x,y,z)\, dz \right] dx\, dy. \qquad (2)$$

Method of calculation

The volumetric mass balance of Glacier de Sarennes has been measured between 1952 and 2003 using aerial photogrammetry. Table 1 gives photogrammetry-related information. In order to orient the images, a stereopreparation was performed in 2005 using geodetic differential GPS (global positioning system) on control points (Fig. 1). Obvious features were used as control points. Moreover, as the relative orientation of the images between the two dates is more important than the absolute ground orientation, nearly 150 tie points on the common 1952 and 2003 bedrock were added to improve consistency. The photogrammetric restitution was performed on a Leica DSR15 analytical plotter with plotted points every 20 m on flat surfaces of the glacier, up to one point per metre in bumpy areas. Then three methods were used to build the DEM: (1) linear interpolations between plotted points, (2) kriging analysis and (3) a triangular irregular network (TIN) based on Delauney's algorithm (Maune, 2007). Each is followed by a re-sampling on a 10 m grid.

The subtraction of the DEMs yields altitudinal variations that must be converted to water equivalent using a density assumption. This can lead to an error which might depend on time, as glaciers losing mass have increasing mean densities and deviate from Sorge's law (Krimmel, 1989). Field data are helpful in investigating the choice of the density function at Sarennes. The 4 years of field mass-balance data available before 1952 reveal a clear negative cumulative budget of –5.99 m w.e. (Valla, 1989). For previous years, meteorological mass-balance computation can be used (Torinesi and others, 2002). We estimate a strong negative cumulative balance of –16 m w.e. for Glacier de Sarennes between 1930 and 1950. Considering the low altitude and the southerly aspect of the glacier, the density of the material that forms its upper layers in 1952 is probably very close to the density of bulk ice. In 2003, the glacier was completely free of snow and firn on the date the

photographs were taken, and it has shown a strong deficit since 1981. We may therefore assume a density of $\rho = 900 \pm (\sigma_\rho = 15)\, kg\, m^{-3}$ in Equation (2) and in all ice-depth to water-equivalent conversions.

The net volumetric mass balance is obtained by dividing the mass variation by a mean surface area, S_m, and is expressed using the height variations of the $Q\ (= 8464)$ nodes of the grid as:

$$b_{vol} = \frac{\Delta m_{vol}}{S_m} = \frac{\rho}{S_m} \sum_{j=1}^{Q} \Delta h_j s_{grid}, \qquad (3)$$

where Δh_j is the altitude variation at node j, and s_{grid} is the elementary surface area of the grid (10 m × 10 m).

Error analysis

Errors are quantified (standard deviation) and combined assuming they are uncorrelated (CETAMA, 1986).

Surface roughness

The surface roughness of the glacier acts as a source of error in stereoscopic measurements. Field observations suggest that surface roughness can be described as waves with peak-to-peak amplitudes, δh_{p-p}, of ∼0.5 m and wavelengths ∼1 to 2 m. As the spatial sampling of the stereoscopic measurement is 20 m, which is one order of magnitude larger than the estimated wavelength, the roughness is analogous to noise in the altitude signal. Assuming a sinusoidal shape for the roughness function (first component of a Fourier series), the standard deviation will be $\sigma_{rgh} = \delta h_{p-p} (\sqrt{2}/2) = 0.35$ m for both years, which is in good agreement with laser-scan values reported for a metric wavelength by Rees and Arnold (2006).

Internal stereoscopic measurement error

The stereoscopic measurement has intrinsic planimetric and altimetric errors which depend on: (1) the scale, s, of the photographs, (2) the sighting error on the stereotypes, σ_{phot}, depending on the visibility of the sighted point, (3) the focal length, T, and (4) the stereoscopic base, B (Kraus and Waldhäusl, 1998). The planimetric error, $\sigma_{stereo.xy}$, is:

$$\sigma_{stereo.xy} = \frac{\sigma_{phot}\sqrt{2}}{s}, \qquad (4)$$

where the sighting uncertainty typically ranges from 10 μm for control and tie points to 30 μm for any point on the surface of the glacier. Similarly, the altimetric error, $\sigma_{stereo.z}$, is:

$$\sigma_{stereo.z} = \frac{T\sigma_{phot}}{s^2 B}. \qquad (5)$$

As explained by Thibert and others (2005), the planimetric error, $\sigma_{stereo.xy}$, also results in an additional altimetric error due to the slope of the ground, given by:

$$\sigma_{stereo.xy} \sqrt{\left(\frac{\partial Z}{\partial x}\right)^2 + \left(\frac{\partial Z}{\partial y}\right)^2}, \qquad (6)$$

where $Z(x,y)$ is the height function provided by the DEM. Using the scale of stereotypes at mean altitudes of the glacier, a mean sighting error of 30 μm and mean slopes of, respectively, 27.7% and 30.6% in 1952 and 2003, planimetric errors of ±1.32 and ±0.87 m are obtained along with a total altimetric error of ±2.10 and ±1.26 m in 1952 and 2003, respectively.

For a single point, the altimetric error accounts for stereoscopic and roughness errors. When repeated every 20 m, the mean error is divided by the square root of the number, P, of sighted points and expressed as the internal altimetric error, σ_z^i:

$$\sigma_z^i = \frac{1}{\sqrt{P}} \sqrt{\sigma_{rgh}^2 + \sigma_{stereo.z}^2 + \sigma_{stereo.xy}^2 \left[\left(\frac{\partial Z}{\partial x}\right)^2 + \left(\frac{\partial Z}{\partial y}\right)^2 \right]}, \tag{7}$$

giving 0.047 (1952) and 0.029 m (2003) using $P = 2116$.

Stereotype orientation error

The absolute orientation of the stereotype itself leads to an error in altitude that does not depend on the number of measurement points. As explained by Thibert and others (2005), errors associated with the absolute orientation of the photographs depend on (1) the height residuals, σ_z, of the ground control points, (2) the planimetric residuals, σ_x, σ_y, which lead to a height error related to the slope of the DEM and (3) the DEM resolution. As shown in this paper, where analogous methods were used to build the DEM, the error related to its resolution appears to be negligible, as the contour lines computed from the DEM merge perfectly with those obtained from the analytical plotter. The overall standard deviation of the height measurement, $\sigma_{a.o}$, associated with the absolute orientation of the photographs is therefore given by:

$$\sigma_{a.o} = \sqrt{\sigma_z^2 + \sigma_x \sigma_y \left[\left(\frac{\partial Z}{\partial x}\right)^2 + \left(\frac{\partial Z}{\partial y}\right)^2 \right]}. \tag{8}$$

Using orientation residuals and mean slopes provided by the DEM, $\sigma_{a.o}$ is 0.34 and 0.22 m in 1952 and 2003, respectively (Table 2).

CORRECTION OF SYSTEMATIC ERRORS

Over and above the random errors detailed in the previous section and the density assumption, the volumetric method also includes systematic errors.

Lack of stereoscopic measurements

The lack of contrast and the evenness of the texture of snow can prevent stereoscopic measurements. In the 1952 photographs this occurs in three regions, of 13.1 ha, of the accumulation zone where altitudes have not been measured but interpolated. Although encircled by reliably measured points, such altitudes are overestimated because concavities are not taken into account by linear interpolations. These altitude differences have been estimated using the concavity of the 2003 DEM where measurements were possible. We found a mean difference in altitude of 1.62 m over 13.1 ha. Considering surface ratios, the overall error on the 1952 DEM is +0.23 m w.e.

Mean surface area used for volume to net balance reduction

For comparison with the balance obtained from field measurements, a water-equivalent balance (b_{vol}) is estimated from Equation (3). The mean surface area (S_m) is generally taken as the arithmetic mean, which can lead to an error, as it assumes that surface and mass balance trends are linear. If both volumetric and glaciological methods provide the same

Table 2. Random and systematic errors in the volumetric and glaciological mass-balance measurements

	1952	2003
Volumetric method		
Random errors		
Surface roughness, σ_{rgh} (m)	0.35	0.35
Planimetric stereoscopic error, $\sigma_{stereo.xy}$ (m)	1.32	0.87
Altimetric stereoscopic error, $\sigma_{stereo.z}$ (m)	2.10	1.26
Internal altimetric error, σ_z^i (m)	0.05	0.03
Orientation residuals σ_x, σ_y, σ_z (m)	0.42, 0.39, 0.32	0.21, 0.21, 0.21
Altimetric orientation error, $\sigma_{a.o}$ (m)	0.34	0.22
Ice density uncertainty, σ_ρ (kg m^{-3})	15	
Mean surface area error, σ_s (km^2)	0.0143	
Error of the volumetric method, σ_{vol} (m w.e.)	1.04	
Systematic errors (m w.e.)		
Lack of stereoscopic measurements	+0.23	0
Volume to net balance reduction	+6% $b_{vol} = +1.94$	
Glaciological method		
Random errors		
Ablation measured in ice, σ_{b-}^{ice} (m w.e. a^{-1})	0.14	
Ablation measured in firn, σ_{b-}^{firn} (m w.e. a^{-1})	0.27	
Accumulation, σ_{b+} (m w.e. a^{-1})	0.21	
Error in firn density, σ_d (m w.e. a^{-1})	5% d ($d = 0.6$; 0.7)	
Mean combined error on all sites (m w.e. a^{-1})	0.097	
Sampling error, σ_{samp} (m w.e. a^{-1})	0.12	
Annual mean error over 51 years (m w.e. a^{-1})	0.16	
Error in cumulative balance, σ_{gla} (m w.e.)	1.15	
Systematic errors (cumulative balance, m w.e.)		
Internal accumulation	–0.22	
Geothermal heat	+0.48	
Water flow*	+0.42	

*Not used to correct the glaciological balance.

measurements, i.e. $\Delta m_{vol} = \Delta m_{gla}$, S_m used in the expression $b_{vol} = \Delta m_{vol}/S_m = \Delta m_{gla}/S_m = \Sigma b_t$ is therefore:

$$S_m = \frac{\sum_{t=1}^{N} b_t S_t}{\sum_{t=1}^{N} b_t}, \tag{9}$$

where b_t denotes the yearly net balances and S_t the surface area of the glacier for year t among the N years (note that if the cumulative mass balance is zero, there is no error associated with the choice of S_m). Evaluating S_m from Equation (9) using field annual mass balances and annual surfaces given by three segmental linear trends between 1952, 1981, 1991 and 2003 (Valla and Piedallu, 1997) gives 0.595 km^2. An arithmetic averaging of 1952 and 2003 surface values gives 0.631 km^2 whereas an arithmetic averaging of segmental linear surfaces gives a higher value of 0.659 km^2. Figure 2 shows the change of S_m with time for intermediate years between 1952 and 2003, together with other surface estimations. Using the 1952–2003 arithmetic mean therefore results in a 6% underestimation of the net balance in absolute values. In order to preserve the independence of both methods, we have nevertheless used this value to calculate the volumetric net balance, and a note of caution should be associated with this choice. The only error that will be considered hereafter in relation to the mean surface is a random error linked to the determination
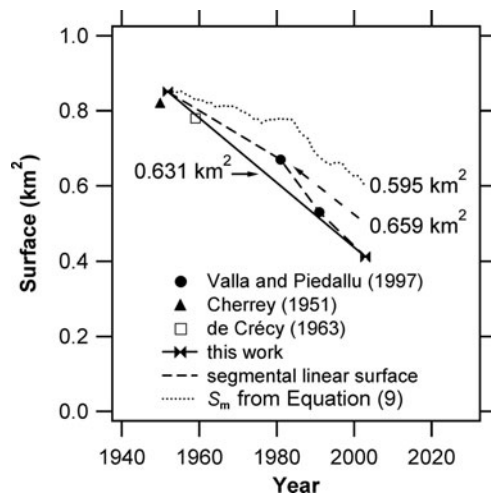
Fig. 2. Surface evolution of Glacier de Sarennes between 1951 and 2003. Possible surface values for net balance reduction from photogrammetry volume changes are indicated.

of the glacier extent on 1952 photographs. Because snow covered the upper part of the glacier, an error of $\pm 0.0286 \, \text{km}^2$ affects its measurement. As this error concerns only 1952, it affects only half of S_m uncertainty. This results in $S_m = 0.6313 \pm (\sigma_s = 0.0143) \, \text{km}^2$.

Results and overall random error

Mass balance

During the 51 years, altitude variations over the glacier range from 0 to $-70 \, \text{m}$ (Fig. 1). The mean altitude variations obtained from the three interpolation methods are very close: $-36 \, \text{m}$ (kriging), $-36.11 \, \text{m}$ (linear interpolation) and $-36.22 \, \text{m}$ (TIN). When analyzing the mean difference between the kriging-interpolated nodes and points measured with the plotter, the linear-interpolation method seems to better fit the source data. In addition, this interpolation provides a balance which is the mean of the three tested methods. Considering that it probably minimizes errors, this method is preferred. The overall error, σ_{vol}, on the volumetric balance is:

$$\sigma_{\text{vol}} = \left\{ b_{\text{vol}}^2 \left(\frac{\sigma_s}{S_m} \right)^2 + b_{\text{vol}}^2 \left(\frac{\sigma_\rho}{\rho} \right)^2 + \left(\rho \frac{Q s_{\text{grid}}}{S_m} \right)^2 \left[\left(\sigma_{z,1952}^i \right)^2 \right. \right.$$
$$\left. \left. + \left(\sigma_{z,2003}^i \right)^2 + \left(\sigma_{\text{a.o},1952} \right)^2 + \left(\sigma_{\text{a.o},2003} \right)^2 \right] \right\}^{1/2} \quad (10)$$

which gives $\pm 1.04 \, \text{m w.e.}$ (surface area, density and photogrammetric errors each contribute nearly a third). Using the correction due to areas without measurement, the volumetric mass balance is $b_{\text{vol}} = -32.30 \pm (\sigma_{\text{vol}} = 1.04) \, \text{m w.e.}$ for the period 1 August 1952 to 20 September 2003.

Mass-balance spatial variability

The overall variability of the mass balance, σ_{sp}, can be calculated from the spatial distribution of altitude changes obtained from photogrammetry (Fig. 1). We assume that the flow of ice is negligible (static glacier) so the water equivalent of the local altitude variation between 1952 and 2003 equals the cumulative local balance. Such an assumption is confirmed by comparing altitude changes given by photogrammetry with local cumulative balances that are negative

over the entire altitude range of the glacier. The discrepancy is very small, $<0.08 \, \text{m w.e. a}^{-1}$ as a mean over the 51 years. Furthermore, the error introduced when assimilating annual height variations, $\partial Z / \partial t$, to the mass balance, $b(x, y)$, can be estimated from the horizontal flux difference over the ice thickness based on the continuity equation (Kääb and Funk, 1999). At a fixed point of the surface in the case of no basal sliding, it can be written as a function of the vertical strain rate ($\dot{\varepsilon}_{zz}$) integration through the ice thickness, h, between the glacier bedrock, Z_0, and the surface Z_s:

$$\frac{\partial Z}{\partial t} - b(x, y) = \int_{Z_0}^{Z_s} \dot{\varepsilon}_{zz} \, \text{d}z \leq h \dot{\varepsilon}_{zz_s} < -h \left(\frac{\partial u_s}{\partial x} + \frac{\partial v_s}{\partial y} \right), \quad (11)$$

where subscript s refers to the glacier surface. An upper limit of the error can therefore be estimated using the vertical strain at the surface, the ice incompressibility, velocities, u_s, v_s, of ablation stakes (0.2–$0.4 \, \text{m a}^{-1}$), slopes provided by the DEM and a mean depth of $45 \, \text{m}$ inferred from Valla and Piedallu (1997). We obtain a small error of $<3 \, \text{cm a}^{-1}$, and therefore consider that the water equivalent of height variations given by photogrammetry are a reliable proxy of the local balance values within the 2003 glacier extent that has been continuously covered by ice since 1952. As a consequence, the overall spatial variability of annual balances is given by the standard deviation of height variations over the 2003 glacier extent which is $\sigma_{\text{sp}} = 0.27 \, \text{m w.e. a}^{-1}$.

GLACIOLOGICAL MASS BALANCE
Data and adjustments

The method used on Glacier de Sarennes measures the yearly net balance (end of ablation season) at five sites using emergence variations of stakes inserted in ice and cores drilled in firn (Fig. 1). Some balances have not been measured, so the experimental table (51 years × 5 sites) is an incomplete set of 243/255 data. Local balances are extrapolated using the area–altitude distribution, which results in a cumulative balance of $-34.62 \, \text{m w.e.}$ (4 September 1952 to 29 September 2003).

For comparison with the volumetric balance, the data have to be adjusted to the same period. Field measurements performed on 23 July and 6 August 1952 can be used to calculate a daily ablation rate close to the date of the aerial photographs (1 August 1952). The adjustment applied to the cumulative balance is then calculated from this rate and from the ablation measured up to the end of the ablation period (20 September 2003). This gives $-0.8 \, \text{m w.e.}$, so the adjusted cumulative balance is $-35.42 \, \text{m w.e.}$ between 1 August 1952 and 20 September 2003, and, considering the adjustment as an additional measurement, the corresponding experimental table is a set of 248/260 data (52 dates × 5 sites).

Random-error analysis

The quantification of the error associated with the glaciological balance requires a distinction between years and sites of negative budget (71%) and those of positive mass balance (29%).

Positive mass balance

Positive balance measurements at the end of the ablation season are based on density and height determinations. These are performed with an auger that provides a single core through the whole depth of the snow.

1. *Density measurement.* Density is mainly affected by the presence of liquid water which may reach up to 20–30% during the ablation period (Vallon and Leiva, 1981) and lead to a 50% overestimation of the density. However, in a summer–autumn firn (density 0.6), as melting ceases, the liquid-water content decreases to reach a non-zero minimum (4%) which depends on the porosity (0.33; Schneider and Jansson, 2004). Such water content represents only 2.4 cm of water for a 1 m depth firn. Densities are therefore not highly affected by the liquid-water content at the end of the ablation season. Errors, mainly related to the size and weight of the cores, have been estimated using another auger (PICO (Polar Ice Coring Office); Kelley and others, 1994) showing that the density is measured within 5%, with no systematic discrepancy. As a result, the uncertainty for firn with a density of 0.6 is $\sigma_d = 0.03$.

2. *Snow height measurement.* The accuracy of the snow height depends on the roughness of the glacier and on the detection of the underlying material. When this material is ice (39 times), the accuracy is generally good, within a few centimetres. When it is firn (33 times), a stratigraphic error is possible despite favourable indicators (hardness, grain size) and can lead to an overestimation of the mass balance if part of the firn of the previous year is accidentally included. Because stratigraphic error is a bias, it has not been included in the present random-error calculation. The overall uncertainty on a positive balance, σ_{b+}, combining density and height contributions is therefore given by:

$$\sigma_{b+} = \sqrt{\sigma_{rgh}^2 d^2 + \sigma_d^2 l^2} \qquad (12)$$

which gives 0.21 m w.e. using $d = 0.6$ and a mean value of snow height of $l = 0.73$ m measured for the 72 positive-balance situations over the period 1952–2003.

Negative mass balance
For a negative budget, the mass balance is measured as an ablation in ice or in firn with an age of 1 year or more.

1. There are 153 ablation values measured as a variation of stake length inserted in ice. The error due to the creep of ice is negligible at Glacier de Sarennes because of the very low flow of ice. Errors are therefore essentially linked to the mechanical play of the jointed stakes and the inaccurate surface at the bottom of stakes due to the anchorage hole. Repeatability tests show that this error is ∼15 cm, which results in an uncertainty of $\sigma_{b-}^{ice} = 0.14$ m w.e. in a balance measured as ablation in ice.

2. The 23 ablation measurements in firn were performed in two ways: (a) with stakes inserted in the underlying ice but emerging from the residual firn of previous year(s) and (b) by drilling in order to reconstruct the stratigraphy when no stakes were found. Errors in observations of type (a) are the same as those for ablation measured in ice (with $d = 0.7$) which gives ±0.11 m w.e. Errors in observations of type (b) are the same as those for positive mass balance but using $l = 0.66$ m as a mean which gives ±0.25 m w.e. Combining the errors from both, σ_{b-}^{firn}, the uncertainty for negative mass balances measured in firn is ±0.27 m w.e.

Sampling error
The finite number of sampling sites results in a sampling error, σ_{samp}, a function of the number of sites, n, and of the overall spatial variability of the mass balance, σ_{sp}, and expressed as:

$$\sigma_{samp} = \frac{\sigma_{sp}}{\sqrt{n}}, \qquad (13)$$

in which σ_{sp} is unknown from the data, but is estimated from photogrammetry. Using a mean value of 4.76 sites sampled each year, this gives a sampling error of ±0.12 m w.e. a^{-1} and results in an error of ±0.89 m w.e. in the cumulative mass balance.

Correction of systematic errors and results
Although negligible on an annual basis, some corrections are required when calculating the cumulative mass balance over decades.

Internal accumulation
Internal accumulation results from the refreezing of percolating water in cold firn and the freezing of capillary-trapped water in snow and firn cooled by the winter cold wave (sensible heat). Both processes are able to account for a significant part of accumulation (Schneider and Jansson, 2004). The occurrence of such processes has been studied using computations developed for Glacier de Saint-Sorlin, which is located at a distance of 3 km (Gerbeaux and others, 2005). These use a mass-balance reconstruction based on the *Crocus* snow model developed by Brun and others (1989). The model estimates a mean sensible heat of 5000 kJ m^{-2} stored each winter in the firn of the accumulation area for the period 1981–2004. Using a specific latent heat of fusion of ice of 335 kJ kg^{-1} (Hobbs, 1974), this results in a mean internal accumulation of 0.015 m w.e. a^{-1} at Glacier de Saint-Sorlin. Using the same mean value at Glacier de Sarennes over the period of record, and an equivalent number of 14 years of positive balance covering the overall glacier, internal accumulation accounts for an underestimate of the mass balance of 0.22 m w.e.

Internal ablation
As ice motion is negligible at Glacier de Sarennes, internal ablation is only caused by two sources of subglacial energy: geothermal heat and heat conversion of the potential energy loss from water flow through and under the glacier.

The geothermal flux is ∼90 mW m^{-2} in this part of the Alps (Gable and Goguel, 1981), which results in a basal melting of 0.94 cm a^{-1}. This ablation rate accounts, consequently, for –0.48 m w.e. over the 51 years of the cumulative balance.

The principle of calculation of ablation from water flow has been described by March and Trabant (1997, equation (9)). Such ablation is divided into two sources. The first is the alpine (non-glacial) runoff over the 0.63 km^2 hydrologic basin. For the 38 years of negative mass balance, melting is estimated from the mean winter balance as 1.60 m w.e. a^{-1}. For the 13 years of positive balance, it is equal to the mean ablation which is 1.50 m w.e. a^{-1}. The second is the glacial runoff over the glacier area (mean 0.63 km^2 over the period), equal to the mean summer balance which is 2.36 m w.e. a^{-1} during 1952–2003.

Assuming that flowing water and ice are at the melting point and form an isolated system, then according to the first
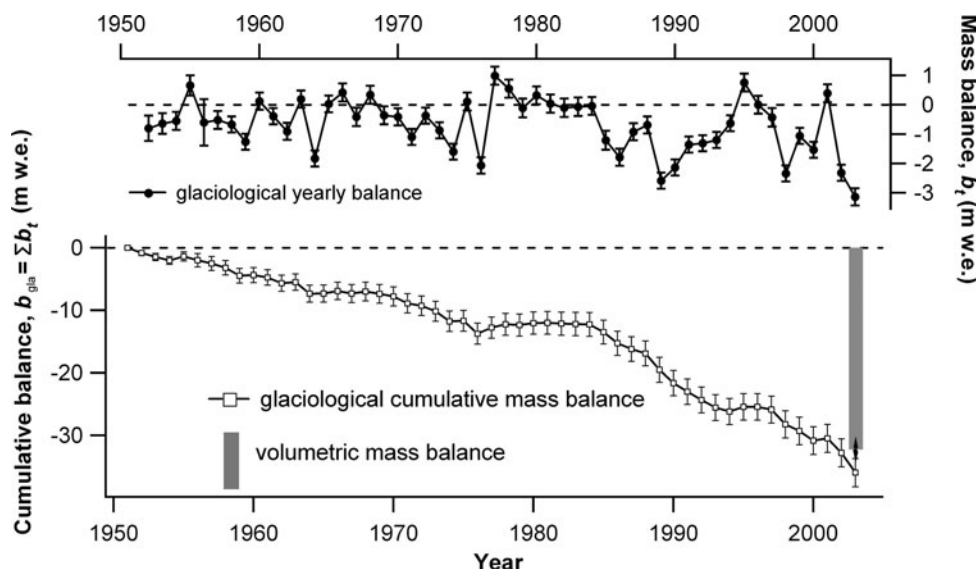
Fig. 3. Glaciological mass balances: upper curve is the glacier-wide yearly balances measured by the glaciological method and its annually calculated random errors according to the type of measurement. Lower curve is the cumulative glaciological mass balance and its comparison to the volumetric balance. No significant discrepancy between the two methods can be admitted at the $\alpha = 5\%$ type I error risk. Error bars are 1.96 standard deviations.

law of thermodynamics, the potential energy lost by water flow is totally converted into heat. Assuming that 100% of the alpine runoff flows under the glacier, the heat per unit area per year can be calculated from the altitude lost by water from the glacier surface to its terminus which is 130 m as obtained from an average 1952–2003 DEM. This gives a heat flux of 158 mW m^{-2}. Nearly half of this is diffused toward the glacier, inducing a melt rate of 0.83 cm a^{-1}, accounting for an ablation of 0.42 m w.e. between 1952 and 2003. This estimation of internal ablation is of the same order of magnitude as ablation due to geothermal heat. However, because it is subject to a number of unverifiable assumptions, such as internal and subglacial water flows, we have not used it to correct the mass balance in the present calculations and prefer to discuss it in the following section.

Updating of the weighting law

As proposed by Cox and March (2004), we have established a linear time-variable area–altitude distribution (AAD) based on 1952 and 2003 DEMs to update the weighting relationship established in 1959 (de Crécy, 1963). The correction to the cumulative mass balance is +0.8 m w.e. (see coefficients in Table 3).

Random uncertainties on point mass balances have been combined in a variance table using the above weighting relationship to give the uncertainty for the whole glacier. It results in an error of 0.7 m w.e. in the cumulative mass balance. Taking into account the sampling error, the error of the cumulative balance is therefore 1.15 m w.e. After correction for the internal accumulation and the geothermal ablation annually distributed, the yearly glacier-wide balance, b_t, is shown in Figure 3. The cumulative balance is $b_{\mathrm{gla}} = \Sigma b_t = -34.89 \pm (\sigma_{\mathrm{gla}} = 1.15)$ m w.e. for the period 1 August 1952 to 20 September 2003.

DISCUSSION

Comparison

The 2.59 m w.e. discrepancy between the two methods is small, representing <10% of the signal. It equals an annual value of less than 6 cm w.e. a^{-1} over 51 years which is far less than the intrinsic random errors of each method. Assuming normally distributed measurements (Fig. 4), in a type I error risk of $\alpha = 5\%$, the discrepancy is not significant, as the condition

$$-1.96\sqrt{\sigma_{\mathrm{gla}}^2 + \sigma_{\mathrm{vol}}^2} < b_{\mathrm{gla}} - b_{\mathrm{vol}} < 1.96\sqrt{\sigma_{\mathrm{gla}}^2 + \sigma_{\mathrm{vol}}^2}$$

is fulfilled by our data, and the hypothesis H$_0$: $b_{\mathrm{vol}} = b_{\mathrm{gla}}$ can therefore be accepted. However, the ability to detect a bias in the glaciological method is given by the test ability to reject H$_0$ when it is actually false. This is the probability of not committing a type II error which is $1 - \beta$ (Table 4). Quantifying β requires choosing the alternative true hypothesis. Assuming that the discrepancy of $\delta b = 2.59$ m w.e. corresponds to a true bias in the glaciological balance,

Table 3. Altitude and area–altitude distribution based weighting coefficients of the five sampling sites in 1952 and 2003. Over the period, coefficients have a linear time variation between initial and final values

Site	Altitude in 2003 (variation since 1952)	Weighting coefficients 1952–2003
	m	%
1	2837* (–51)	3.5–0
2	2887 (–61)	3–18
3	2922 (–49)	15–38.5
4	2978 (–40)	35.5–25.5
5	3001 (–35)	42–18

*As the glacier retreat from site 1 occurs during summer 2003, the altitude is that of bedrock.

Table 4. Type I and II errors associated with the detection of a significant discrepancy between glaciological and volumetric balances. From our data, the tested hypothesis, H_0: $b_{vol} = b_{gla}$, is not rejected at the $\alpha = 5\%$ type I probability of error. However, if H_0 is false, and the true hypothesis is $b_{gla} = b_{vol} + 2.59$ m w.e., there is a probability of $\beta = 61.4\%$ of a wrong acceptance of H_0

True hypothesis	Outcome of the test	
	$b_{gla} = b_{vol}$ rejected	$b_{gla} = b_{vol}$ accepted
$b_{gla} = b_{vol}$	wrong conclusion $\alpha = 5\%$*	right conclusion $1 - \alpha = 95\%$*
$b_{gla} = b_{vol} + 2.59$ m w.e.	right conclusion $1 - \beta = 38.6\%$[†]	wrong conclusion $\beta = 61.4\%$[†]

*Type I error fixed at $\alpha = 5\%$.
[†]Resulting type II error from fixed alternative hypothesis and $\alpha = 5\%$ type I error.

β will then be

$$\beta = F\left(1.96 - \frac{\delta b}{\sqrt{\sigma_{gla}^2 + \sigma_{vol}^2}}\right) - F\left(-1.96 - \frac{\delta b}{\sqrt{\sigma_{gla}^2 + \sigma_{vol}^2}}\right), \quad (14)$$

where F is the repartition function of the normal law, so that it results in a high risk of a wrong conclusion with $\beta = 61.4\%$. This shows that there is a low probability (38.6%) of making the correct selection in this case. This is mainly due to the high common standard deviation of both methods (1.55 m w.e.) which reaches 40% of the measured discrepancy.

We may therefore ask, with fixed type I and II errors, what the detectable bias, δb, is. This is given by

$$\delta b = \left(u_{1-\frac{\alpha}{2}} - u_{1-\beta}\right)\sqrt{\sigma_{gla}^2 + \sigma_{vol}^2}, \quad (15)$$

where u_γ is given by the normal distribution law as $F(u_\gamma) = \gamma$. For $\alpha = \beta = 5\%$ admissible errors, δb is 5.6 m w.e. (0.11 m w.e. a^{-1}; Fig. 4). For $\alpha = \beta = 10\%$, δb is 0.06 m w.e. a^{-1}. These biases are smaller than the mean annual random error of the glaciological balance (0.16 m w.e. a^{-1}) and therefore are very difficult to detect, showing that the ability of the volumetric method to test field data is not all that important. Moreover, corrections of results from the estimation of possible systematic errors are critical to support any conclusions derived from the comparison. If corrected for all possible and quantifiable biases (volume to net balance reduction, subglacial melting from water flow), the discrepancy would be 1.07 m w.e., giving $\beta = 75\%$. If present in the glaciological balance, biases are low and therefore cannot be reliably detected and quantified by such a comparison. However, a variance analysis allows the extraction of spatial effects from field data and the potential systematic errors remaining to be quantified. This is the topic of the next subsection.

Variance analysis

The natural spatial variability of the mass balance is a potential source of systematic error through an erroneous weighting relationship or insufficient spatial sampling. Considering that it is estimated from photogrammetry as
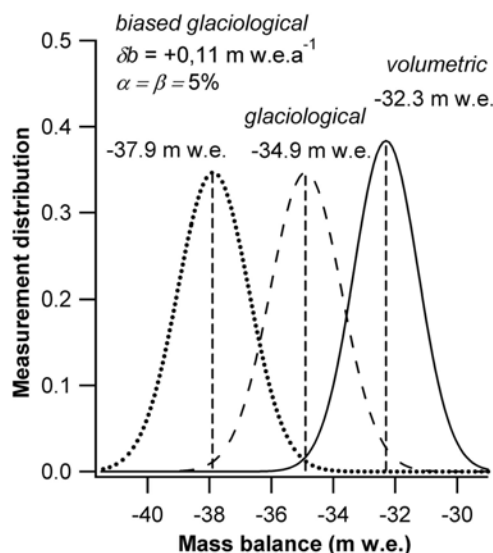

Fig. 4. Normal distribution of results. The solid curve is the volumetric mass balance and the dashed curve is the glaciological mass balance. The dotted curve is the lowest detectable biased glaciological mass balance for 5% type I and II error risks.

0.27 m w.e. a^{-1}, it is important to check whether field data hold all or part of this variability. This can be performed with the variance analysis proposed by Lliboutry (1974). By comparison with more descriptive analyses such as principal components, a variance analysis allows an explicit separation of overall space and time effects, non-linear effects and random errors, at the cost of a hypothesis of identically centred and normally distributed residuals and temporal control factors.

The model specifies that $b_{i,t}$, the mass balance recorded at stake i for year t and corrected by the systematic annual bias, is decomposed in four terms as:

$$b_{i,t} = \alpha_i + \beta_t + \gamma_i \delta_t + \varepsilon_{i,t}. \quad (16)$$

The α_i terms are mean annual balances at each stake, and their standard deviation is the spatial variability of the data. The β_t term represents an amount of mass balance, constant over all the glacier, which differs from year to year. Under the constraint $\sum \beta_t = 0$, β_t is called the centred mass balance and can be interpreted as the annual and uniform response of all stakes to climate fluctuations. The cross-term, $\gamma_i \delta_t$, under the constraints $\sum \gamma_i = 0$ and $\sum \delta_t = 0$, represents additional effects that deviate from the time and space variability separation. The $\varepsilon_{i,t}$ term represents residuals corresponding to both measurement errors and discrepancies between the model and data. Variances, σ_α, σ_β and σ_δ, need to be estimated together with the missing values of the experimental table. Inference is carried out in a Bayesian framework using a Markov chain Monte Carlo scheme (Gilks and others, 1996).

The variance analysis results are presented in Table 5. The modelling hypotheses are not rejected at good confidence levels by standard tests such as Snedecor's and χ^2 on the period of record (51 years, 5 stakes and 12 missing values). In particular, the hypothesis of identically normally distributed residuals is fulfilled, indicating that a variance-analysis model is well suited to the studied glacier. The standard deviation of the residual is 0.24 m w.e. a^{-1}, which is just slightly greater than the mean measurement error at
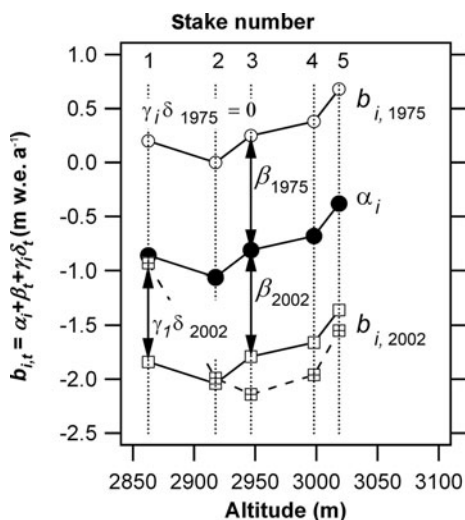
Fig. 5. Variance decomposition (α_i, β_t, $\gamma_i\delta_t$) of balances, $b_{i,t}$, through the linear model (see text).

Table 5. Variance analysis results for the glaciological mass-balance data over the period 1952–2003 (values in m w.e.)

	$b_{i,t} = \alpha_i + \beta_t + \gamma_i\delta_t + \varepsilon_{i,t}$	
Variability source	Mean	Standard deviation
α_1	-0.87 ± 0.03	
α_2	-1.10 ± 0.03	
α_3	-0.85 ± 0.04	
α_4	-0.71 ± 0.03	
α_5	-0.39 ± 0.04	
Overall spatial, α_i	-0.79 ± 0.11	0.26 ± 0.08
Temporal, β_t	$\sum \beta_t = 0$	0.94 ± 0.09
Non-linear, $\gamma_i\delta_t$	$\sum \delta_t = \sum \gamma_i = 0$	0.17 ± 0.09
Residual, $\varepsilon_{i,t}$	–	0.24 ± 0.02

each stake (± 0.17 m w.e. a^{-1}) and indicates that the model fits well the space and time variability of the data.

Three main conclusions result from this variance analysis.

1. Regarding the temporal variability, the balance at each stake differs from year to year by an amount which is nearly uniform over the entire glacier. This is shown in Figure 5, where the mean balance measured over the period of record at each stake is plotted versus altitude (α_i curve). Yearly net balances are simply shifted with the β_t annual value from the α_i spatial distribution curve (as plotted for the year 1975). This linear shift fits 94.5% of the data. This linear behaviour has been reported for other glaciers (Meier and Tangborn, 1965; Llibouotry, 1974; Kuhn 1984; Rasmussen, 2004) and is not surprising for Glacier de Sarennes which is a small size glacier with a small altitude range. However, non-linear effects explain some of the variability of the data, as 14 cross-terms among 255 are significantly different from 0 at the 95% confidence level. Figure 5 illustrates this for stake 1 in 2002 where a cross-term, $\gamma_1\delta_{2002}$, must be added to correctly fit the data. Note that non-linearity does not play any role in the quantification of the space and time effects because of the modelling constraints, and a pure linear model would have led to the same α_i and β_t.

2. Regarding the spatial variability, the deviation from the mean glaciological balance caused by the sampling at five sites is significant, showing that sampling on more than one is worthwhile (Table 5). However, sampling on four sites would be acceptable, as the discrepancy between the α_i spatial terms is not significant for stakes 1 and 3. The standard deviation between the α_i is 0.26 m w.e. a^{-1} and therefore very close to the 0.27 m w.e. a^{-1} overall spatial variability estimated from photogrammetry. This point suggests that all the spatial variability is recorded by the adopted sampling.

3. The final point is related to the linear composition of time and space variabilities. It results in only needing one stake to record the annual β_t deviation which is the same at each stake. This can also be shown by the very high stake-to-stake (>69%) and stake-to-β_t (>85%) correlations. Best estimators are stakes 2 and 4, as the data from each

explain 97% and 96% of β_t, respectively. Nevertheless, the number of sites should not be reduced excessively. Firstly, despite low spatial variability and small differences between the α_i, their distribution is needed to calculate the glacier-wide balance. Secondly, random errors related to the sampling and to point measurements are divided by the square root of the number of sites. Thirdly, the risk of losing some data increases for a low number of sites (stake not found or broken). Even if the linear model makes it possible to estimate missing values in the experimental table, at least one is needed every year, and the standard deviation while estimating β_t is higher for years with missing values.

To complete the assessment regarding possible sources of systematic errors, the reliability of the spatial integration must be considered. The low spatial variability of the mass balance estimated from photogrammetry (0.27 m w.e. a^{-1}) is reasonable given the small size and small altitude range (165 m) of the glacier. Small size and altitude range result in a reduced sensitivity of the glacier-wide balance to variable weighting parameters: using the same weight at each site would have led to a cumulative mass balance different by 4.5 m w.e. over 51 years which corresponds to <0.09 m w.e. a^{-1}. This suggests that any systematic error in the weighting law, if it exists, would not be significant.

Nevertheless, given that the occurrence of such a systematic error cannot be totally ruled out and that the true distribution of the mass balance over the glacier is unknown, preference is given to photogrammetry to estimate the cumulative glacier-wide balance. The cumulative balance (adjusted to 4 September 1952 to 29 September 2003) that we recommend is therefore –31.5 m w.e. ($\pm\sqrt{\sigma_{vol}^2 + \sigma_{b+}^2 + (\sigma_{b-}^{ice})^2} = \pm 1.07$ m w.e.). Regarding yearly balances, it seems also preferable to combine both methods. As α_i terms represent mean annual balances at each stake, the best possible estimate of their spatial integration is given by the mean annual volumetric balance, which is $b_{vol}/N = -0.62$ m w.e. a^{-1} over the adjusted period. Considering that the α_i to altitude correlation is poor ($r^2 = 0.42$), this seems more reliable than using the AAD integration relationship. Glacier-wide balance, b_t, can therefore be expressed for any years of the period by:

$$b_t = \frac{b_{vol}}{N} + \beta_t, \tag{17}$$

where β_t is the centred mass balance obtained from the variance analysis (Table 6).

CONCLUSION AND RECOMMENDATIONS

The purpose of this paper is to compare glaciological and volumetric mass-balance methods in search of systematic errors. When corrected for biases due to quantifiable systematic errors, the two measurements differ by only 2.59 m w.e. and no significant discrepancy can be detected at the 95% confidence level (type I error). However, the hypothesis that the discrepancy is linked to a systematic difference can only be accepted at a confidence level of 39% (type II error). Nevertheless, even if they are hardly detectable in the glaciological balance, potential residual systematic errors seem to be small. A variance analysis shows that the spatial sampling of field data covers the low overall spatial variability of the mass balance (0.27 m w.e.) over the small (0.5 km^2) Glacier de Sarennes. All the spatial information is therefore accounted for by sampling sites.

As a result of the comparison and the variance analysis, the two methods should be considered complementary, and we propose to combine them in future work according to the following recommendations:

1. The investigation of climate variations requires the extraction of the centred mass balance, β_t, which accounts for the temporal variability and is free of effects related to the geometry and the dynamics of the glacier. This should be based on a variance analysis of the glaciological balance data, with a linear separation of spatial and temporal variables. Such a variance analysis also makes it possible to discard superfluous stakes and retain a reduced network. Although not discussed in the present paper, both winter and summer balances may be analyzed this way (Rasmussen and Andreassen, 2005).

2. Given that the occurrence of systematic errors in the glaciological method cannot be totally ruled out, we recommend using photogrammetry to find the cumulative balance over a long period of monitoring. We conclude that the cumulative balance for Glacier de Sarennes is –31.5 (±1.07) m w.e., when adjusted to the end of both ablation seasons (4 September 1952 to 29 September 2003), and that the best possible estimate of yearly glacier-wide balances is a combination of the photogrammetric mean annual balance (–0.62 m w.e. a^{-1}) and the centred mass balance resulting from the variance analysis.

Table 6. Centred mass balance, β_t, estimated from variance analysis, and glacier-wide balance, b_t, combining photogrammetry and variance analysis using Equation (17) over the period 1952–2003

Year	β_t	b_t
	m w.e.	m w.e.
1952/53	-0.24 ± 0.14	-0.86
1953/54	-0.31 ± 0.12	-0.93
1954/55	1.41 ± 0.12	0.79
1955/56	0.11 ± 0.24	-0.51
1956/57	-0.07 ± 0.12	-0.69
1957/58	-0.06 ± 0.10	-0.68
1958/59	-1.00 ± 0.10	-1.62
1959/60	0.75 ± 0.10	0.13
1960/61	0.19 ± 0.10	-0.43
1961/62	-0.19 ± 0.10	-0.81
1962/63	0.75 ± 0.10	0.13
1963/64	-1.42 ± 0.10	-2.04
1964/65	0.72 ± 0.10	0.10
1965/66	1.14 ± 0.11	0.52
1966/67	0.33 ± 0.10	-0.29
1967/68	1.05 ± 0.10	0.43
1968/69	0.24 ± 0.10	-0.38
1969/70	0.37 ± 0.11	-0.25
1970/71	-0.54 ± 0.11	-1.16
1971/72	0.26 ± 0.11	-0.36
1972/73	0.02 ± 0.10	-0.60
1973/74	-0.86 ± 0.10	-1.48
1974/75	0.90 ± 0.10	0.28
1975/76	-1.38 ± 0.10	-2.00
1976/77	1.62 ± 0.10	1.00
1977/78	1.27 ± 0.10	0.65
1978/79	0.46 ± 0.10	-0.16
1979/80	1.09 ± 0.10	0.47
1980/81	0.79 ± 0.10	0.17
1981/82	0.58 ± 0.10	-0.04
1982/83	0.52 ± 0.10	-0.11
1983/84	1.09 ± 0.11	0.47
1984/85	-0.33 ± 0.10	-0.95
1985/86	-1.14 ± 0.11	-1.76
1986/87	-0.25 ± 0.10	-0.87
1987/88	0.09 ± 0.10	-0.53
1988/89	-1.79 ± 0.10	-2.41
1989/90	-1.41 ± 0.11	-2.03
1990/91	-0.58 ± 0.11	-1.20
1991/92	-0.67 ± 0.10	-1.29
1992/93	-0.68 ± 0.10	-1.30
1993/94	0.13 ± 0.10	-0.49
1994/95	1.49 ± 0.10	0.87
1995/96	0.93 ± 0.10	0.31
1996/97	0.06 ± 0.10	-0.56
1997/78	-1.56 ± 0.10	-2.18
1998/99	-0.46 ± 0.11	-1.08
1999/2000	-0.79 ± 0.10	-1.41
2000/01	1.09 ± 0.10	0.47
2001/02	-1.13 ± 0.11	-1.75
2002/03	-2.55 ± 0.12	-3.17

REFERENCES

Andreassen, L.M. 1999. Comparing traditional mass balance measurements with long-term volume change extracted from topographical maps: a case study of Storbreen glacier in Jotunheimen, Norway, for the period 1940–1997. *Geogr. Ann.,* **81A**(4), 467–476.

Bader, H. 1954. Sorge's Law of densification of snow on high polar glaciers. *J. Glaciol.,* **2**(15), 319–323.

Braithwaite, R.J. 1986. Assessment of mass-balance variations within a sparse stake network, Qamanârssûp sermia, West Greenland. *J. Glaciol.,* **32**(110), 50–53.

Braithwaite, R.J., T. Konzelmann, C. Marty and O.B. Olesen. 1998. Errors in daily ablation measurements in northern Greenland, 1993–94, and their implications for glacier climate studies. *J. Glaciol.,* **44**(148), 583–588.

Brun, E., E. Martin, V. Simon, C. Gendre and C. Coléou. 1989. An energy and mass model of snow cover suitable for operational avalanche forecasting. *J. Glaciol.,* **35**(121), 333–342.

CETAMA (Commission d'Établissement des Méthodes d'Analyses du Commissariat à l'Énergie Atomique). 1986. *Statistique appliquée à l'exploitation des mesures. Second edition.* Paris, Masson.

Cherrey, M. 1951. Observations d'octobre 1949 à octobre 1950 du glacier de Sarennes. *Mémoires et travaux de la section de glaciologie.* Grenoble, Société Hydrotechnique de France, 3–10. (Numéro spécial A.)

Cogley, J.G. and W.P. Adams. 1998. Mass balance of glaciers other than the ice sheets. *J. Glaciol.,* **44**(147), 315–325.

Cox, L.H. and R.S. March. 2004. Comparison of geodetic and glaciological mass-balance techniques, Gulkana Glacier, Alaska, USA. *J. Glaciol.,* **50**(170), 363–370.

de Crécy, L. 1963. Le glacier de Sarennes et le climat grenoblois. *Annales de l'Ecole Nationale des Eaux et des Forêts et de la Station de Recherches et Expériences,* **20**(3), 345–370.

Dyurgerov, M.B. and M.F. Meier. 1999. Analysis of winter and summer glacier mass balances. *Geogr. Ann.,* **81A**(4), 541–554.

Fountain, A.G. and A. Vecchia. 1999. How many stakes are required to measure the mass balance of a glacier? *Geogr. Ann.,* **81A**(4), 563–573.

Gable, R. and J. Goguel. 1981. Carte du flux géothermique. *In* Souquet, P., *ed. Structure et dynamique de la lithosphère, Vol. 2.* Toulouse, Centre Régional de Documentation Pédagogique de Midi-Pyrénées.

Gerbaux, M., C. Genthon, P. Etchevers, C. Vincent and J.P. Dedieu. 2005. Surface mass balance of glaciers in the French Alps: distributed modeling and sensitivity to climate change. *J. Glaciol.,* **51**(175), 561–572.

Gilks, W.R., S. Richardson and D.J. Spiegelhalter., *eds.* 1996. *Markov chain Monte Carlo in practice.* London, Chapman and Hall.

Haeberli, W. 1996. Glacier fluctuations and climate change detection. *Geogr. Fís. Din. Quat.,* **18**(2), 191–199.

Hobbs, P.V. 1974. *Ice physics.* Oxford, etc., Clarendon Press.

Kääb, A. and M. Funk. 1999. Modelling mass balance using photogrammetric and geophysical data: a pilot study at Griesgletscher, Swiss Alps. *J. Glaciol.,* **45**(151), 575–583.

Kelley, J.J., K. Stanford, B. Koci, M. Wumkes and V. Zagorodnov. 1994. Ice coring and drilling technologies developed by the Polar Ice Coring Office. *Mem. Nat. Inst. Polar Res.* 49, Special Issue, 24–40.

Kraus, K. and P. Waldhäusl. 1998. *Manuel de photogrammetrie. Principes et procédés fondamentaux.* Paris, Edition Hermès.

Krimmel, R.M. 1989. Mass balance and volume of South Cascade Glacier, Washington, 1958–1985. *In* Oerlemans, J., *ed. Glacier fluctuations and climatic change.* Dordrecht, etc., Kluwer Academic Publishers, 193–206.

Krimmel, R.M. 1999. Analysis of difference between direct and gerdetic mass balance measurements at South Cascade Glacier, Washington. *Geogr. Ann.,* **81A**(4), 653–658.

Kuhn, M. 1984. Mass budget imbalances as criterion for a climatic classification of glaciers. *Geogr. Ann.,* **66A**(3), 229–238.

Le Meur, E. and C. Vincent. 2003. A two-dimensional shallow ice-flow model of Glacier de Saint-Sorlin, France. *J. Glaciol.,* **49**(167), 527–538.

Lliboutry, L. 1974. Multivariate statistical analysis of glacier annual balances. *J. Glaciol.,* **13**(69), 371–392.

March, R.S. and D.C. Trabant. 1997. Mass balance, meteorological, ice motion, surface altitude, and runoff data at Gulkana Glacier, Alaska, 1993 balance year. *USGS Water-Resour. Invest. Rep.* 96-4299.

Maune, D., ed. 2007. *Digital Elevation Model technologies and applications: the DEM user's manual. Second edition.* Bethesda, MD, American Society for Photogrammetry and Remote Sensing.

Meier, M.F. and W.V. Tangborn. 1965. Net budget and flow of South Cascade Glacier, Washington. *J. Glaciol.,* **5**(41), 547–566.

Meier, M.F., W.V. Tangborn, L.R. Mayo, and A. Post. 1971. Combined ice and water balances of Gulkana and Wolverine Glaciers, Alaska, and South Cascade Glacier, Washington, 1965 and 1966 hydrologic years. *USGS Prof. Pap.* 715-A.

Oerlemans, J. and J.P.F. Fortuin. 1992. Sensitivity of glaciers and small ice caps to greenhouse warming. *Science,* **258**(5079), 115–117.

Østrem, G. and N. Haakensen. 1999. Map comparison or traditional mass-balance measurements: which method is better? *Geogr. Ann.,* **81A**(4), 703–711.

Rasmussen, L.A. 2004. Altitude variation of glacier mass balance in Scandinavia. *Geophys. Res. Lett.,* **31**(13), L13401. (10.1029/2004GL020273.)

Rasmussen, L.A. and L.M. Andreassen. 2005. Seasonal mass-balance gradients in Norway. *J. Glaciol.,* **51**(175), 601–606.

Rees, W.G. and N.S. Arnold. 2006. Scale-dependent roughness of a glacier surface: implications for radar backscatter and aerodynamic roughness modelling. *J. Glaciol.,* **52**(177), 214–222.

Schneider, T. and P. Jansson. 2004. Internal accumulation in firn and its significance for the mass balance of Storglaciären, Sweden. *J. Glaciol.,* **50**(168), 25–34.

Thibert, E., J. Faure and C. Vincent. 2005. Bilans de masse du Glacier Blanc entre 1952, 1981 et 2002 obtenus par modèles numériques de terrain. *Houille Blanche,* **2**, 72–78.

Torinesi, O., A. Letréguilly and F. Valla. 2002. A century reconstruction of the mass balance of Glacier de Sarennes, French Alps. *J. Glaciol.,* **48**(160), 142–148.

Valla, F. 1989. Forty years of mass-balance observations on Glacier de Sarennes, French Alps. *Ann. Glaciol.,* **13**, 269–272.

Valla, F. and C. Piedallu. 1997. Volumetric variations of Glacier de Sarennes, French Alps, during the last two centuries. *Ann. Glaciol.,* **24**, 361–366.

Vallon, M. and J.C. Leiva. 1981. Bilans de masse et fluctuations récentes du Glacier de Saint-Sorlin (Alpes Francaises). *Z. Gletscherkd. Glazialgeol.,* **17**(2), 143–167.

Vincent, C. 2002. Influence of climate change over the 20th century on four French glacier mass balances. *J. Geophys. Res.,* **107**(D19), 4375. (10.1029/2001JD000832.)